DC mobilization from the skin requires docking to immobilized CCL21 on lymphatic endothelium and intralymphatic crawling

Orna Tal,[1] Hwee Ying Lim,[2] Irina Gurevich,[1] Idan Milo,[1] Zohar Shipony,[1] Lai Guan Ng,[3] Veronique Angeli,[2] and Guy Shakhar[1]

[1]Department of Immunology, Weizmann Institute of Science, Rehovot 76100, Israel
[2]Department of Microbiology, Immunology Programme, Yoon Loo Lin School of Medicine, National University of Singapore, Singapore, 117456
[3]Singapore Immunology Network, Agency for Science, Technology and Research, Biopolis, Singapore, 117597

Dendritic cells (DCs) must travel through lymphatics to carry skin antigens into lymph nodes. The processes controlling their mobilization and migration have not been completely delineated. We studied how DCs in live mice respond to skin inflammation, transmigrate through lymphatic endothelium, and propagate in initial lymphatics. At steady state, dermal DCs remain sessile along blood vessels. Inflammation mobilizes them, accelerating their interstitial motility 2.5-fold. CCR7-deficient BMDCs crawl as fast as wild-type DCs but less persistently. We observed discrete depositions of CCL21 complexed with collagen-IV on the basement membrane of initial lymphatics. Activated DCs move directionally toward lymphatics, contact CCL21 puncta, and migrate through portals into the lumen. CCR7-deficient DCs arrive at lymphatics through random migration but fail to dock and transmigrate. Once inside vessels, wild-type DCs use lamellipodia to crawl along lymphatic endothelium and, sensing lymph flow, proceed downstream. DCs start drifting freely only in collecting lymphatics. These results demonstrate in vivo that the CCL21–CCR7 axis plays a dual role in DC mobilization: promoting both chemotaxis and arrest of DCs on lymphatic endothelium. Intralymphatic crawling, in which DCs combine active adhesion-based migration and directional cues from lymph flow, represents a new step in DC mobilization which may be amenable to regulation.

CORRESPONDENCE
Guy Shakhar:
shakhar@weizmann.ac.il

Abbreviations used: BMDC, BM-derived DC; CHS, contact hypersensitivity; DDC, dermal DC; LC, Langerhans cell; LEC, lymphatic endothelial cell; LYVE1, lymphatic vessel hyaluronan receptor 1; QD, quantum dot; SNARF, seminaphtharhodafluor; VE-cadherin, vascular endothelial cadherin.

To efficiently initiate immune responses to skin pathogens, migratory DCs capture antigens, undergo maturation, and enter lymphatic vessels leading them into LNs (Banchereau and Steinman, 1998). Although the migration of skin DCs to LNs is critical for most vaccination procedures (Romani et al., 2010), the sequence of events regulating their mobilization has not been delineated fully.

DCs in the mammalian skin can be broadly divided into two populations: Langerhans cells (LCs) in the epidermis, and dermal DCs (DDCs) in the dermis (Merad et al., 2008; Bedoui et al., 2009). Recent findings have used combinations of the markers CD103, CD207, and CD11b to further divide DDCs into subpopulations, each specializing in immune responses against different pathogens (Bedoui et al., 2009; Brewig et al., 2009).

For many years, LCs had been considered the major population of antigen-presenting cells to prime immune responses against skin antigens. More recently, the deeper and scarcer DDCs emerged as central players. They are the first cells to appear in draining LNs carrying antigen from the skin (Kamath et al., 2002; Itano et al., 2003; Kissenpfennig et al., 2005), were found to be more motile than LCs in situ (Lindquist et al., 2004; Kissenpfennig et al., 2005; Ng et al., 2008), and proved superior in priming certain immune responses (Helft et al., 2010). The present study focuses on this key population of skin DCs.

Under inflammatory conditions, skin DCs, and first among them DDCs, are recruited to

O. Tal and H. Ying Lim contributed equally to the paper

The Rockefeller University Press $30.00
J. Exp. Med. Vol. 208 No. 10 2141-2153
www.jem.org/cgi/doi/10.1084/jem.20102392

The Journal of Experimental Medicine

the LNs en masse. This recruitment depends on a cascade of events that starts as keratinocytes and skin leukocytes recognize microbial ligands using their pattern recognition receptors, proceeds as they secrete inflammatory mediators such as leukotrienes, prostaglandins, and cytokines, and continues as lymphatic endothelial cells (LECs) release chemokines and DCs change their chemokine receptor profile (Randolph et al., 2005; Alvarez et al., 2008).

A pivotal chemokine receptor is CCR7, which is upregulated by migratory DCs and acts as a gatekeeper of their mobilization (Dieu et al., 1998; Saeki et al., 1999). As corroborated in knockout mice, without engagement of CCR7 DCs do not enter lymphatics and do not appear in LNs several hours later (Förster et al., 1999; Martín-Fontecha et al., 2003; Ohl et al., 2004). Complementary roles in DC mobilization have been suggested for CCR8-CCL1 (Qu et al., 2004), CXCR4-CXCL12 (Kabashima et al., 2007), and S1P-S1P1/3 signaling (Czeloth et al., 2005), but CCR7 seems to play the most central role.

The chemokines CCL21 (of which several variants exist) and CCL19 are the known ligands of CCR7. Based on work in mice deficient in these chemokines, CCL21 seems more important than CCL19 to mobilize skin DCs to LNs (Randolph et al., 2005; Britschgi et al., 2010). In contrast to CCL19, which is fully soluble, CCL21 has a heparan sulfate–binding domain which promotes its immobilization to various membranal and matrix proteins (Patel et al., 2001; Kerjaschki et al., 2004; Yang et al., 2007).

The prevailing model has long been that $CCR7^+$ DCs arrive at initial lymphatic vessels by migrating up a chemotactic gradient of CCL19 and CCL21 secreted by the lymphatic vessels themselves (Saeki et al., 1999). This scenario, though, has not been demonstrated directly (Swartz et al., 2008). Recently, Schumann et al. (2010) demonstrated that DCs require both the immobilized form of CCL21 and the soluble form of CCL21, which they cleave off the immobilized form, to optimally spread and migrate in vitro. It was not revealed if this mechanism operates in the more complex in vivo milieu or would pertain to DC recruitment into lymphatics.

The microanatomical structure of initial lymphatics supports leukocyte entry. In the dermis, lymphatics form a flat network that runs beneath the epidermis. The lymphatic capillaries are blind ended, have a flattened cross section, and are sheathed with a discontinuous basal membrane containing collagen IV (Pflicke and Sixt, 2009). The gaps in this membrane, termed portals, serve as entry points for DCs to squeeze through and reach the lymphatic endothelium (Pflicke and Sixt, 2009). LECs display oak leaf morphology and adjoin each other through discrete cell junctions, termed buttons, interspersed by loose flaps (Baluk et al., 2007). The molecular composition of buttons resembles vascular adherens junctions and tight junctions, with an important component being vascular endothelial cadherin (VE-cadherin), which maintains their structural integrity (Baluk et al., 2007). Based on examination of tissue explants, DCs are believed to enter lymphatics by displacing the flaps into the lymphatic lumen while the buttons remain in position and act as hinges (Pflicke and Sixt, 2009). How CCR7 signaling is incorporated into this complex microanatomical setup remains unknown.

Unlike the entry of leukocytes into lymphatic capillaries, a process which is beginning to be unraveled, little is known about the mode of DC propagation inside these vessels. The simplest scenario suggests that DCs are passively swept along the lymph flow (Alvarez et al., 2008). This mode of transport would mimic the fast drift of tumor cells in tumor-draining lymphatics, which was observed in vivo by several groups (Dadiani et al., 2006; Hayashi et al., 2007), and could explain the presence of free-floating veiled DCs in lymph fluid harvested from afferent lymphatics (Kelly et al., 1978). It is yet unclear, though, whether the narrow cross section of initial lymphatics and the hydrodynamic forces that prevail inside them would support such motion. Notably, within inflamed venules, which, like initial lymphatics, are narrow and slow flowing, leukocytes use an elaborate array of chemokines and adhesion molecules to interact with the endothelium, crawl, and extravasate (Ley et al., 2007).

As initial lymphatics converge into collecting vessels, DCs would be expected to drift passively inside them. Secondary collecting lymphatics are sectioned into rhythmically contracting lymphangions separated by valves. These structures actively pump lymph toward the draining LN (Swartz et al., 2008) at velocities sufficient to carry cells (Dadiani et al., 2006; Hayashi et al., 2007).

In recent years, multiphoton imaging in live animals has revealed how leukocytes travel in lymphoid tissues and target organs (Germain et al., 2006). Researchers captured DCs as they migrate in the skin (Lindquist et al., 2004; Ng et al., 2008; Pflicke and Sixt, 2009; Sen et al., 2010) and in LNs (Lindquist et al., 2004; Miller et al., 2004) but have not applied this method to the question of DC propagation in lymphatics (Cavanagh and Weninger, 2008) and the role of specific chemokine receptors. In this paper, we aim to examine DCs in the skin of live mice and address the following questions: (a) whether DDCs occupy a defined niche in the skin and how they respond to skin inflammation; (b) what anatomical route DCs follow to access lymphatics and where along this route CCL21-CCR7 signaling regulates DCs recruitment; and (c) how DCs propagate inside lymphatics and what role lymph flow plays in directing this migration.

RESULTS

To investigate how DCs migrate in the skin and mobilize, we modified a method for noninvasive imaging of the hind footpad in anesthetized mice (Zinselmeyer et al., 2008). We visualized endogenously fluorescent DDCs or adoptively transferred BM-derived DCs (BMDCs), and their interaction with lymphatics (immunolabeled in vivo) using two-photon intravital microscopy.

Choosing the footpad allowed us to immobilize it under a chamber while maintaining normal blood flow, tissue oxygenation, and body temperature. Imaging this area has the

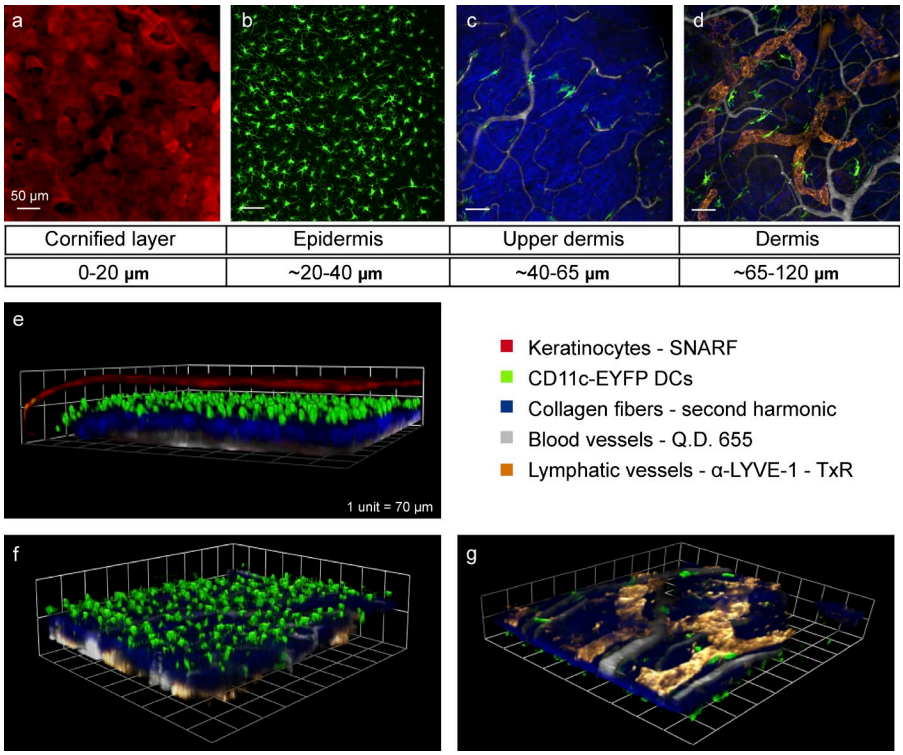

Figure 1. Optical sectioning of the intact footpad skin from a live CD11c-EYFP mouse. (a–d) Images representing extended focus views of subsequent layers. (a) The upper layer of the epidermis, at 0–20 µm in depth, consists of cornified keratinocytes stained topically with SNARF. (b) The epidermis, at ~20–40 µm, contains CD11c-EYFP$^+$ star-shaped LCs. (c) The upper dermis, at ~40–65 µm, contains collagen fibers, which generate a second harmonic signal, and blood vessels traced with QD655. (d) The deeper dermis, at ~65–120 µm, contains CD11c-EYFP$^+$ DDCs and lymphatics stained with anti-LYVE1 conjugated to Texas Red. (e–g) Three-dimensional reconstructions of all the above layers (e), epidermal LCs (f), and dermal lymphatics, DDCs and blood vessels shown from below (g). Images are representative of at least 15 paws of CD11c-EYFP$^+$ mice examined.

advantages of not requiring hair removal, less autofluorescence and photodamage in melanocytes and hair follicles, and simplified DC transfer.

DCs populations in the footpad skin

Using CD11c–enhanced (E) YFP mice, whose DCs, but not other cell types, express high levels of EYFP (Lindquist et al., 2004), we could visualize the skin down to the s.c. space (located ~120 µm deep), revealing all the epidermal and dermal layers (Fig. 1 and Video 1). Topical staining with the vital dye seminaphtharhodafluor (SNARF) revealed the stratum corneum composed of cornified keratinocytes (Fig. 1, a and e). About 20 µm deeper into the epidermis resided flat highly branched EYFP$^+$ cells, representing the LC population (Fig. 1, b and f). LCs were evenly spaced at a mean density of ~1,000 cells/mm^2 and sent delicate dendrites from the cell soma. As expected, no blood or lymph vessels penetrated this layer. About 40 µm beneath the surface (Fig. 1 c), in the upper dermis, a basement membrane composed of collagen fibers was clearly visible based on second harmonic generation. This layer was traversed by blood capillaries which we traced with quantum dot (QD) 655 nanoparticles. CD11c-EYFP$^+$ DDCs first appeared at this depth, most of which adjoined blood vessels at a mean density of ~60 cells/mm^2. Scanning deeper into the dermis (~65 µm below the surface), lymphatic vessels first appeared (Fig. 1, d and g). These were intertwined with blood vessels and exhibited a wider cross section and a simpler branched morphology. Lymphatics were stained by s.c. injection of antibody against lymphatic vessel hyaluronan receptor 1 (LYVE1), a surface marker not involved in DC migration (Gale et al., 2007). DDCs in this layer were amoeboid in their morphology, far sparser than LCs (at around 110 cells/mm^2), and heterogeneously distributed, with higher densities around blood vessels (Fig. 2 a). We are currently investigating the biological function of this unexpected association with blood vessels. Whole-mount staining confirmed the presence of CD11c-EYFP^{hi} MHC-II$^+$ cells in this layer (Fig. S1). Hereafter, we focused on the dermal layer, dynamically imaging the interactions between DDCs and lymphatics.

Quiescent DCs are mobilized in response to inflammation

To begin assessing the response of DDCs to inflammation, we compared intact skin with skin injected with CFA 18–24 h earlier. We tracked the three-dimensional motion of the cells (Fig. 2, a–d; and Video 2) and quantified their velocity and arrest coefficient (which is the proportion of time that a cell is not crawling; Fig. 2, e and f). At steady state, DDCs exhibited relatively little translational movement (0.78 µm/min on average). Local application of CFA accelerated DDCs almost 2.5-fold (Fig. 2 e), up to 2.06 µm/min ($P < 0.001$), and decreased their arrest coefficient from 0.80 to 0.61 ($P < 0.001$; Fig. 2 f). Similarly motile CD11c-EYFP$^+$ DCs were observed in injured skin (Video 3).

CCR7 signaling takes part in DC recruitment, participating in chemotaxis and, more critically, in DC docking to the lymphatic endothelium

After inflammation, CD11c-EYFP$^+$ DDCs entered initial lymphatics and could be observed crawling inside them (Video 4). Nonetheless, cell numbers were low and we rarely captured events of trans-endothelial migration. To observe significant numbers of entry events, and to use genetically manipulated

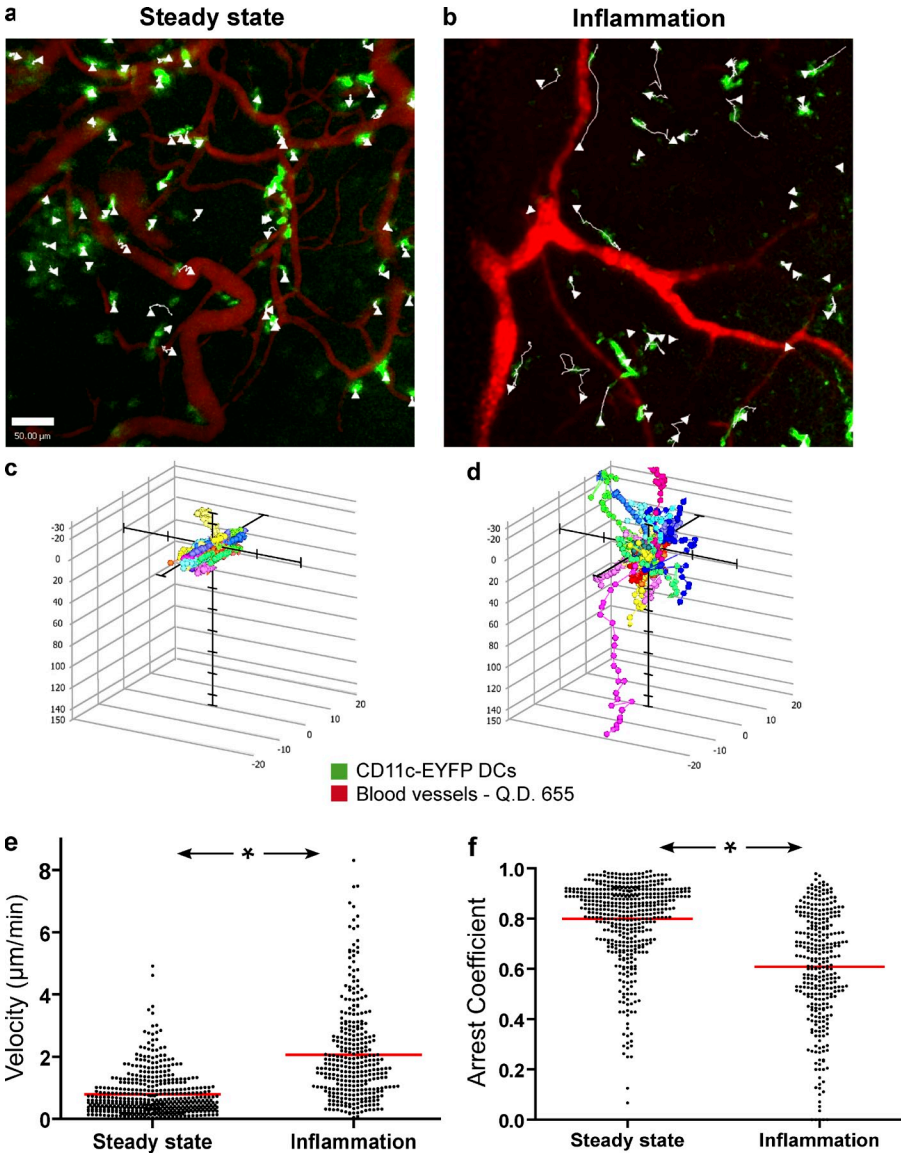

Figure 2. Inflammation of the footpad accelerates DDC movement in the dermis. (a and b) Extended focus snapshots of the dermis in the steady-state (a) or 24 h after injecting CFA s.c. (b). Tracks show the motion of selected DDCs through 45 min (arrowheads indicate the endpoints of tracked cells). (c and d) Charts representing the three-dimensional paths, normalized to their starting coordinates, taken by the cells tracked above. (e and f) Crawling velocities (e) and arrest coefficients (f). Shown is the percentage of time in which cells were immobile (slower than 2 µm/min). Data points represent individual cells (*n* of steady state = 535, *n* of CFA-treated = 305) and were pooled from six mice and 15 movies for each condition. Red bars denote the mean. Inflammation increased velocities and reduced arrest. *, $P < 0.0001$ for both.

DCs in wild-type hosts, we proceeded to use adoptive transfer of BMDCs. These cells resemble the monocyte-derived DCs used in vaccination trials in cancer patients. Understanding the migration requirements of such cells is important because, when injected to the skin in clinical trials, typically <5% of them reach the draining LNs (De Vries et al., 2003).

DC mobilization is a multistep process that is tightly controlled by CCR7 signaling. We set out to determine at what stages of DC mobilization CCR7 acts as a gatekeeper. We reasoned that: (a) If CCR7 signaling is required for DC chemokinesis, then $CCR7^{-/-}$ DCs should exhibit reduced motility in the dermis; (b) if it is essential to chemoattract DCs, then $CCR7^{-/-}$ DCs should not reach the lymphatics vessels; (c) if it is required for adherence to lymphatic endothelium, then they would reach the lymphatics but ignore them, continuing to migrate in the dermis; (d) if it is required for trans-endothelial migration, then DCs would accumulate outside lymphatics on the basal surface of their endothelium; and finally, (e) if it is required for crawling inside lymphatics, then they should accumulate on the luminal surface.

To examine these possibilities, we s.c. injected the footpads of wild-type host mice with fluorescently labeled BMDCs of either WT or $CCR7^{-/-}$ origin. Suspensions containing 3×10^6 BMDCs were injected together with 50 ng LPS, and the dermis was imaged 18–24 h later. The motion of WT DCs toward lymphatics showed indications of chemotaxis; because DCs were injected s.c., most cells approached lymphatics from below (Video 5, right square) but when cells moved parallel to the surface, they could be tracked displaying linear motion toward the nearest lymphatic (Fig. 3 b; and Video 5, left). Within 24 h, 95% of WT cells in the imaged fields successfully transmigrated into the lymphatic lumen (Fig. 3 d and Video 6), whereas <5% of $CCR7^{-/-}$ DCs did so (Fig. 3 e and Video 6). Similar results were obtained when both DC population were co-injected into the same host (Fig. 3 f and Video 7). Notably, about half of the $CCR7^{-/-}$ cells were observed brushing against lymphatics but failing to arrest and enter them (Fig. 3 e, tracked cells; and Video 6). In the dermal interstitium, WT and $CCR7^{-/-}$ DCs moved at similar velocities (6.37 vs. 7 µm/min, $P = 0.29$), but $CCR7^{-/-}$ DCs followed more tortuous pathways as reflected in a lower persistence index ($P = 0.006$; Fig. 3, g and h). This implies that CCR7 signaling is not essential for DC chemokinesis but participates in their chemotaxis. Correspondingly, $CCR7^{-/-}$ DCs did not demonstrate linear motion toward the nearest lymphatics.

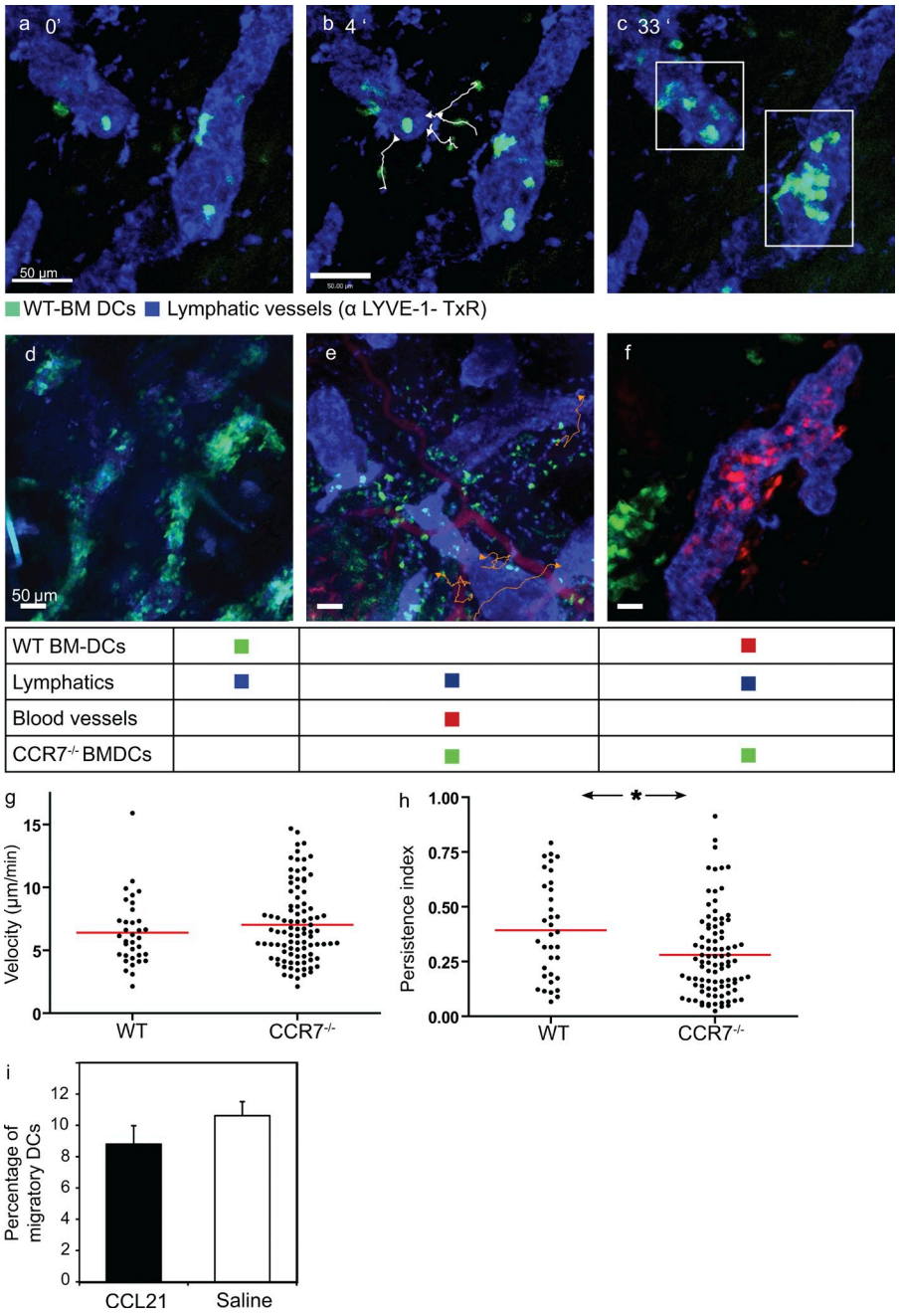

Figure 3. CCR7 plays a dual role in DCs mobilization, promoting chemotaxis and docking to lymphatics. After s.c. injection of LPS-activated CFSE-stained BMDCs to the footpad, WT DCs (a–c) moved linearly toward an initial lymphatic, compatible with chemotaxis. DCs that crossed the endothelium clustered in the proximal sections of initial lymphatics, either in blind ends (c, left rectangle) or in adjacent sections (c, right rectangle). (d) Within 24 h, WT cells have efficiently entered lymphatics. In contrast, CCR7$^{-/-}$ cells (e) kept crawling in the interstitium bypassing the lymphatic vessels they encountered (four representative cells tracked), suggesting that CCR7 promotes DC adhesion to lymphatics. This pattern was also apparent (f) when both WT and CCR7$^{-/-}$ DCs were co-injected. CCR7$^{-/-}$ DCs crawled as fast as WT DCs in the dermis ($P = 0.29$; g) but were less persistent ($P = 0.006$; h), implying that CCR7 ligation is not essential for DC chemokinesis but participates in their chemotaxis. Persistence index was calculated by dividing the cell displacement by path length. Data points represent individual cells and were pooled from three mice for each condition. Red bars denote the mean. *, $P = 0.006$. (i) When BMDCs were co-injected with CCL21, their migration to the popliteal LN was not affected, indicating that misplaced chemokine did not misguide DCs and prevent random migration and docking on endothelial CCL21. Data indicate the percentage of injected DCs out of resident LN CD11c^{+} cells. Error bars denote SEM.

To verify that immobilized CCL21 can trigger DC adhesion, rather than chemokinesis, we studied the behavior of WT and CCR7$^{-/-}$ BMDCs in a flow chamber coated with CCL21. Unlike CCR7$^{-/-}$ cells, WT DCs settled the surface, spread, and exhibited tight adhesion under flow conditions. Adhesion likely depended on inside-out activation of β-2 integrins because it was abolished in the absence of Mg^{+2} ions (unpublished data).

To establish whether CCL21 injected together with DCs would reduce their migration into the LNs by chemotactically directing them away from lymphatics, we co-injected BMDCs with 2.5 μg CCL21. The migration of DCs did not change significantly (Fig. 3 i) compared with saline-injected footpads. Collectively, these results suggest that CCR7 ligands play a dual role, first in chemotaxis, and then, more critically, in DC docking to the lymphatic endothelium.

CCL21 shows a unique punctate expression pattern on LECs

The finding that CCR7-dependent docking was crucial for DC mobilization into lymphatics prompted us to investigate whether DCs in the dermis contact the CCR7 ligand CCL21 on the initial lymphatics themselves. We used confocal microscopy to examine whole-mount skin samples from the footpad and ear either at steady state or after inflammation induced by contact hypersensitivity (CHS) or CFA. Staining for LYVE-1 and CCL21 revealed that CCL21 was not uniformly distributed along the LECs but concentrated on discrete regions of the cells (Fig. 4 a). A similar pattern was visible in skin samples from footpads (Fig. 4 a)

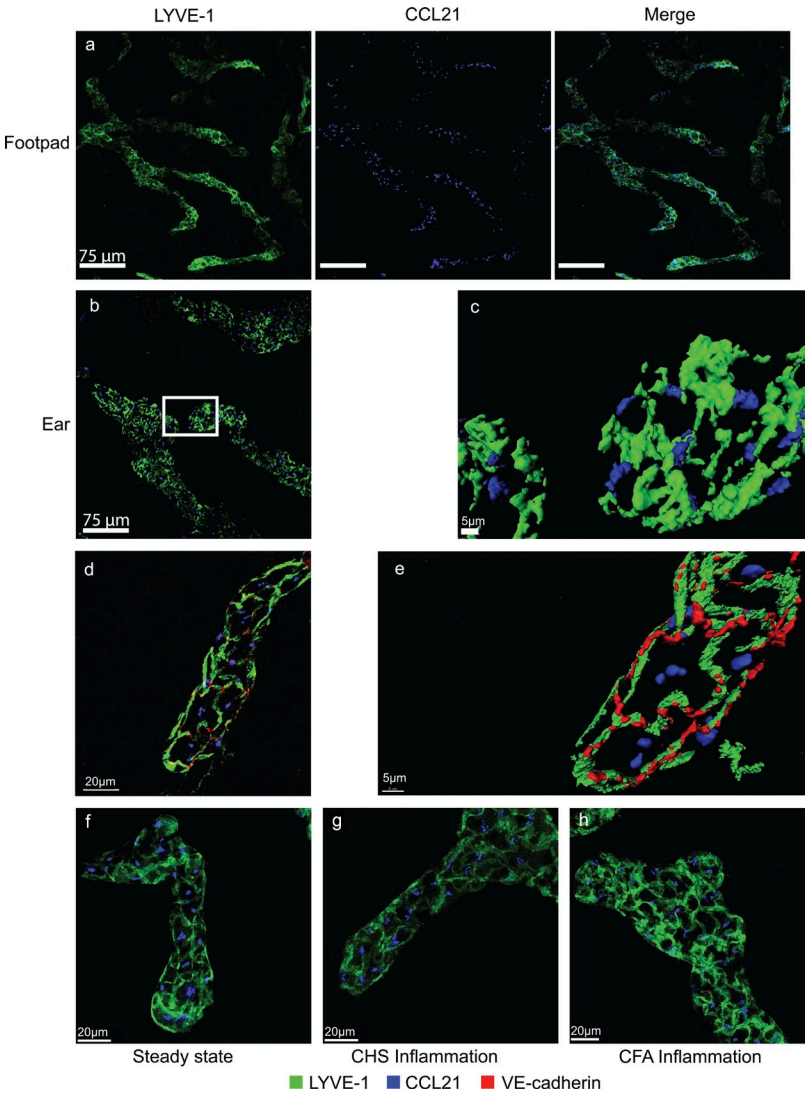

Figure 4. CCL21 depositions are concentrated in specific regions of LECs. Whole-mount confocal images of the skin of the footpad (a) or ear (b) stained for LYVE-1 and CCL21 showed a punctate expression of CCL21 on initial lymphatics (blue dots). (c) This pattern was even more obvious after isosurface rendering. (d and e) Triple staining for VE-cadherin, LYVE-1, and CCL21 shows alternate arrangement of VE-cadherin at button junctions and LYVE-1 at loose flaps. CCL21 puncta are located in the junction-free areas of the LECs. (f–h) Compared with the steady-state, inflammation, either through CHS (g) or CFA (h), did not affect the pattern of CCL21 puncta or increase the CCL21 signal after 24 h.

and ears (Fig. 4 b). The punctuate distribution of CCL21 on initial lymphatics was particularly conspicuous after three-dimensional isosurface rendering of confocal image stacks (Fig. 4 c).

LECs in initial lymphatics are joined by button junctions that contain VE-cadherin and are interspaced by flaps that allow cellular transmigration (Pflicke and Sixt, 2009). Triple staining of initial lymphatics for VE-cadherin, CCL21, and LYVE-1 (Fig. 4, d and e) showed that CCL21 did not colocalize with VE-cadherin in buttons. Instead, CCL21 concentrations lied close to, but not within, the LYVE-1–positive flaps. This location suggests that CCL21 promotes the docking of DCs to the endothelium rather than their subsequent transmigration through the flaps. Interestingly, compared with the steady state (Fig. 4 f), skin inflammation, either through CHS (Fig. 4 g) or CFA (Fig. 4 h), did not enhance CCL21 puncta nor disrupted their pattern, although it did increase the flow of lymph to the draining LN (Fig. S2).

CCL21 ligation may help DCs traverse the basement membrane and interact with LECs

The recent observation that before entering initial lymphatics DCs traverse the basement membrane through preformed portals (Pflicke and Sixt, 2009) raises the possibility that CCL21 is associated with these sites. We visualized the portals in the basement membrane by staining whole mounts of ear skin for collagen IV. The basement membrane of initial lymphatics was indeed perforated and, interestingly, we found that CCL21$^+$ puncta were associated with these perforations in >95% of the cases (Fig. 5, a and b). Moreover, treating skin samples with collagenase type IV, in the presence of calcium, effectively dissociated the majority of CCL21 from initial lymphatics, supporting the association of CCL21 with collagen IV at the basement membrane of the vessels (Fig. 5, c and d).

We next examined the interaction of endogenous DDCs identified by MHC class II (Fig. 5, e–h) or EYFP expression (Fig. 5, i–l) with CCL21$^+$ regions of initial lymphatics in the ear skin. 24 h after induction of inflammation, endogenous DCs preferentially clustered around the proximal portion of the vessel. More to the point, some DCs that approached the CCL21$^+$ lymphatics extended protrusions toward them and contacted the chemokine puncta (Fig. 5, e–l; and Video 8), likely allowing them to attach to the vessels. Altogether, these results further support a novel role of CCR7-CCL21 signaling in mediating docking of DCs to initial lymphatics, which is a requirement for subsequent transmigration.

DCs transmigrate through the endothelium of initial lymphatics and accumulate in selected sections

After docking to the abluminal surface of lymphatics, DCs (either endogenous or transferred and imaged as described in the previous section) typically did not crawl along the abluminal surface of the endothelium before starting to transmigrate (Fig. 3 a and Video 5). Within 30 min of docking, DCs succeeded to penetrate the lumen, where they were released (Fig. 6 a and Video 9).

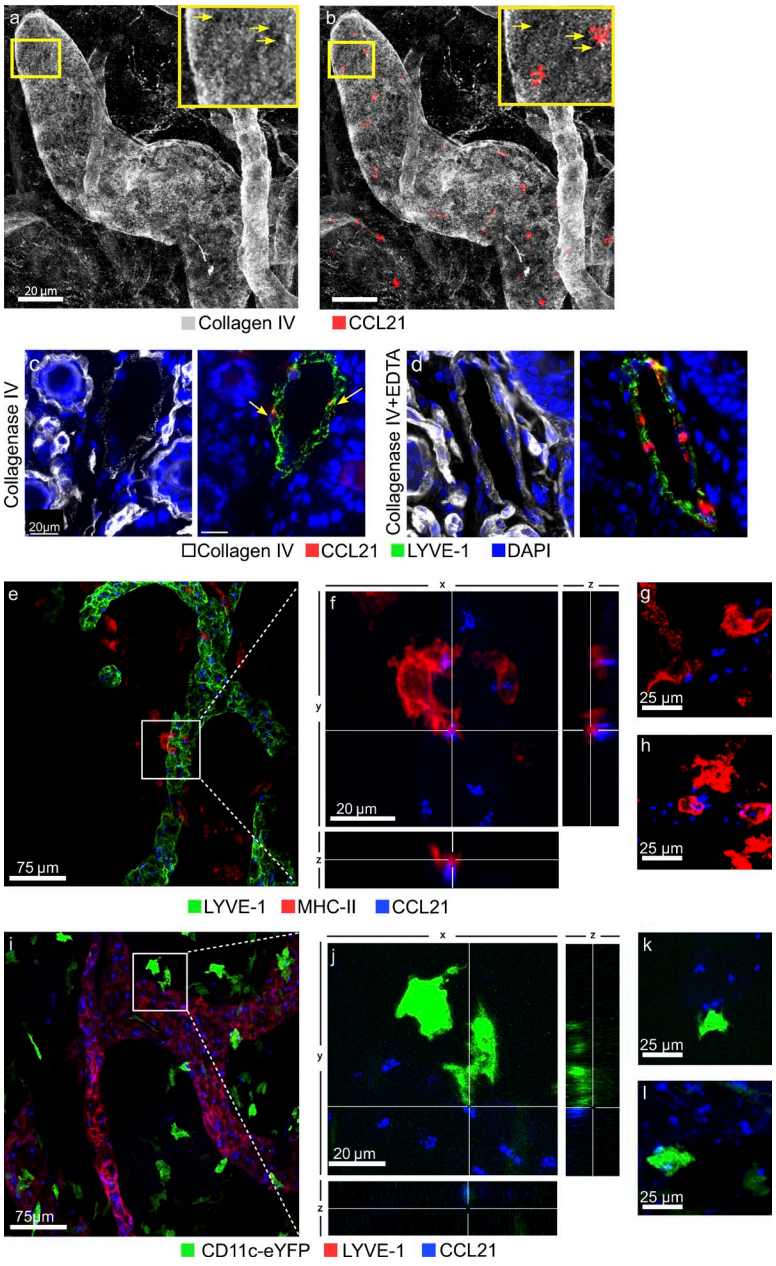

Figure 5. CCL21 immobilization on the basement membrane of initial lymphatics may facilitate DC adhesion at CCL21-rich sites and passage through dedicated portals. (a) Collagen IV staining in whole-mount preparations of the ear skin shows perforations within the basement membrane of initial lymphatics (arrows in boxed region). (b) CCL21 staining reveals that several, but not all, of these perforations (arrows) are associated with CCL21 puncta. (c) Treatment of skin cross sections with type IV collagenase digested the basal membrane of initial lymphatics, markedly reducing collagen on lymphatics. Membrane-bound CCL21was dissociated, leaving behind small perinuclear depositions (arrows). (d) In the presence of the calcium chelator EDTA, collagenase IV treatment did not disrupt collagen (left) and CCL21 (right). (e–h) 24 h after contact sensitization, skin whole mounts were triple-stained for LYVE-1, CCL21, and MHC-II. MHC-II$^+$ DCs accumulated outside initial lymphatics (e). (f) Enlargement of the boxed region in e shows in three dimensions a DC which extended protrusions toward the initial lymphatic vessel and contacted two CCL21-rich puncta. Two other examples of DCs contacting CCL21 are shown (g and h). (i–l) Similar results were obtained when the skin of CD11c-EYFP mice was analyzed. Collectively, these findings suggest that CCL21 is secreted from intracellular stores inside LECs and is immobilized on the basal membrane (often near preformed portals), to promote DC adhesion and site-specific transmigration.

DCs tended to cross the endothelium at preferred sections of the initial lymphatics and clustered before releasing (Fig. 3 c and Video 5). Clustering occurred at the blind ends of lymphatics, or immediately downstream, but not further along the vessels. On several occasions we observed two DCs successively transmigrating through the exact same points (Fig. 6 b and Video 10), likely representing the aforementioned portals (Pflicke and Sixt, 2009).

The mode of DC propagation in initial lymphatics is active crawling

DCs that have entered initial lymphatics need to migrate directionally to reach the draining LN. We expected the lymph flow to sweep the cells downstream as soon as they enter the lymphatics. Instead, we observed that they actively crawled inside the lymphatic lumen (Fig. 7 a and Video 11), advancing at a slow mean velocity of 7.75 µm/min. The flattened cross section of initial lymphatics permitted DCs to maintain close contact with both the bottom and top luminal surfaces of these vessels and crawl by extending filopodia at their leading edges and exhibiting clear uropods at their trailing edges (Fig. 7 b). Similar behavior was exhibited by endogenous CD11c-EYFP$^+$ DDCs (Video 4). Cells occasionally reversed their polarization (Video 11) and traveled back and forth in the lymphatics, or even lodged into the blind end. This irregular motion exhibited itself in a relatively low mean persistence index of 0.36.

The nondirectional movement of DCs inside the lymphatics seemed counterintuitive, as such random motility would delay their arrival to the LN. We suspected that anesthesia had decreased the flow of lymph in the initial lymphatics and compromised DC migration. Various anesthetics have long been known to reduce lymph flow by abolishing voluntary muscle movements, reducing muscle tone, and decreasing lymphangion contraction (Schmid-Schönbein, 1990).

To test this possibility we s.c. injected 4×10^6 GFP$^+$ DCs to the footpads of awake or continuously anaesthetized mice and harvested their popliteal LNs 10 h later. Anesthesia reduced the percentage of newly migrating DCs fivefold ($P < 0.001$), lending credibility to our hypothesis (Fig. 7 c).

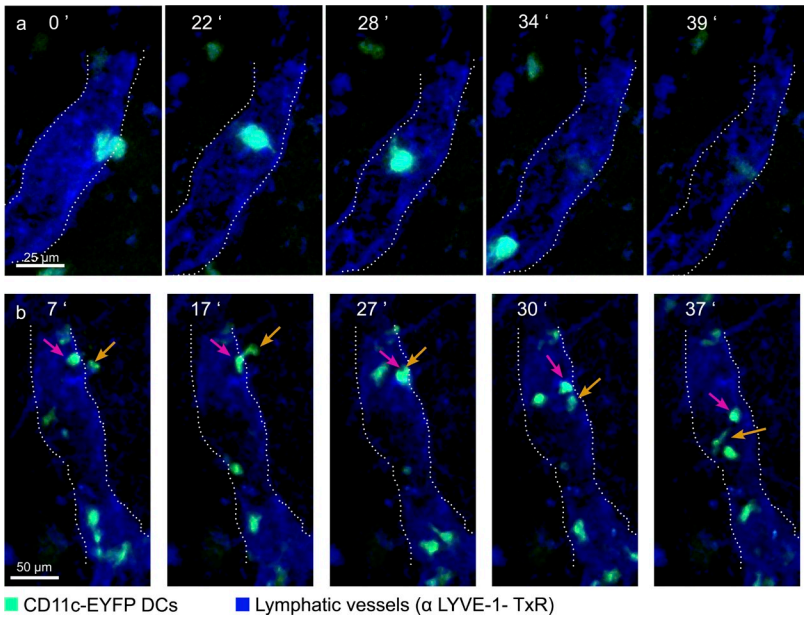

Figure 6. DCs trans-migrate through the endothelium in selected lymphatic sections. The footpad was injected with BMDCs s.c. with 24 h before imaging. (a) Sequential images (timed 0–40 min) demonstrate the typical dynamics of DC transmigration; within 20 min, a DC that adhered to abluminal surface of a lymphatic vessel trans-migrated into the lymphatic lumen and started crawling. (b) Two DCs cross through the same spot on the endothelium, presumably representing a preformed portal (Pflicke and Sixt, 2009).

Next we studied how lymph flow affects the motility of DCs inside lymphatics. Because it has been shown that elevated interstitial flow increases lymph flow and DC migration to LNs (Miteva et al., 2010), we manipulated lymph flow by artificially increasing the pressure of the interstitial fluid. After locating transferred DCs inside initial lymphatics, we s.c. injected 5–10 µl of PBS containing a fluorescent tracer (QD655) and followed the motion of the DCs (Fig. 7 d and Video 12). The fluid could be observed diffusing through the dermal interstitium and concentrating in initial lymphatics. DCs responded to the flow by propagating toward the LN. Although their crawling velocity remained constant at ∼8 µm/min, their persistence index increased from 0.375 to 0.65 as they started moving linearly along the vessel. Cell morphology and speed indicated that DCs remained in close contact with the endothelium throughout this process. When mice were anesthetized with isoflurane, which is believed to interfere less with lymph flow (Video 13), cells showed a propensity to crawl directionally toward LNs, but still crawled in close contact with the lymphatic endothelium.

DCs flow passively in collecting lymphatics

As expected, in the faster-flowing collecting lymphatics, DCs drifted passively rather than crawling actively. We could observe cells drifting at high speeds in the large collecting and afferent lymphatics leading to the popliteal LN (Fig. S3 a). Measurements revealed speeds of ∼1,200 µm/min, which is ∼200-fold faster than the maximal crawling speed recorded in the initial lymphatics. In accordance with previous results (Lindquist et al., 2004), once inside the draining LN the transferred DCs dispersed in the subcapsular sinus (Fig. S3 b and Video 14) before migrating into the T cell zone.

DISCUSSION

We have followed the multistep journey of DCs from the inflamed skin to the draining LN. In the intact dermis, most DDCs adhered to blood vessels and showed little movement. After sensing an inflammatory signal, DCs accelerated 2.5-fold and patrolled the dermis. Ligation of CCR7 on DCs allowed them to dock to punctate CCL21 depositions on the abluminal surface of initial lymphatics and enter them, most likely through dedicated portals. In contrast, CCR7-deficient DCs crawled as rapidly but less persistently in the dermis, contacting lymphatics but failing to dock and transmigrate. Once inside initial lymphatics, DCs used their lamellipodia to interact with the endothelium, and, guided by the direction of lymph flow, polarized and actively crawled toward the draining LN. After reaching collecting lymphatics, DCs started drifting freely in the lymph flow.

Two recent studies described how CD11c-EYFP$^+$ DDCs in the ear respond to inflammatory agents (Ng et al., 2008; Sen et al., 2010). The DDCs recorded by Sen et al. (2010) were initially sessile and accelerated in response to a skin irritant or to adjuvants. In contrast, Ng et al. (2008) found that DDCs crawled constantly in the steady state and stopped in response to systemic LPS administration or to local Leishmania infection. Here, we studied DDC dynamics in the footpad skin and found that CFA-mediated inflammation mobilized the normally sessile DDCs. The disagreement between our data and those of Ng et al. (2008) may be explained by the different skin areas examined (footpad and ear, respectively) or the depth at which cells were recorded; the present study examined DDCs in the deep dermis, whereas the ear model investigated DDCs in the upper dermis. The DDCs in our footpad preparation responded to inflammation like those studied by Sen et al. (2010) in the ear. But for unknown reasons this group could not identify DDCs in the footpad, so the data cannot be directly compared.

The physiological importance of chemotaxis toward soluble chemokines is a long-standing question (Proudfoot et al., 2003) that we address here in the context of lymphatic intravasation under inflammation. CCR7 ligands were initially envisioned as soluble chemoattractants released to promote DC motility and attract them to lymphatics (Saeki et al., 1999). Mounting in vitro evidence, however, suggests that CCL21

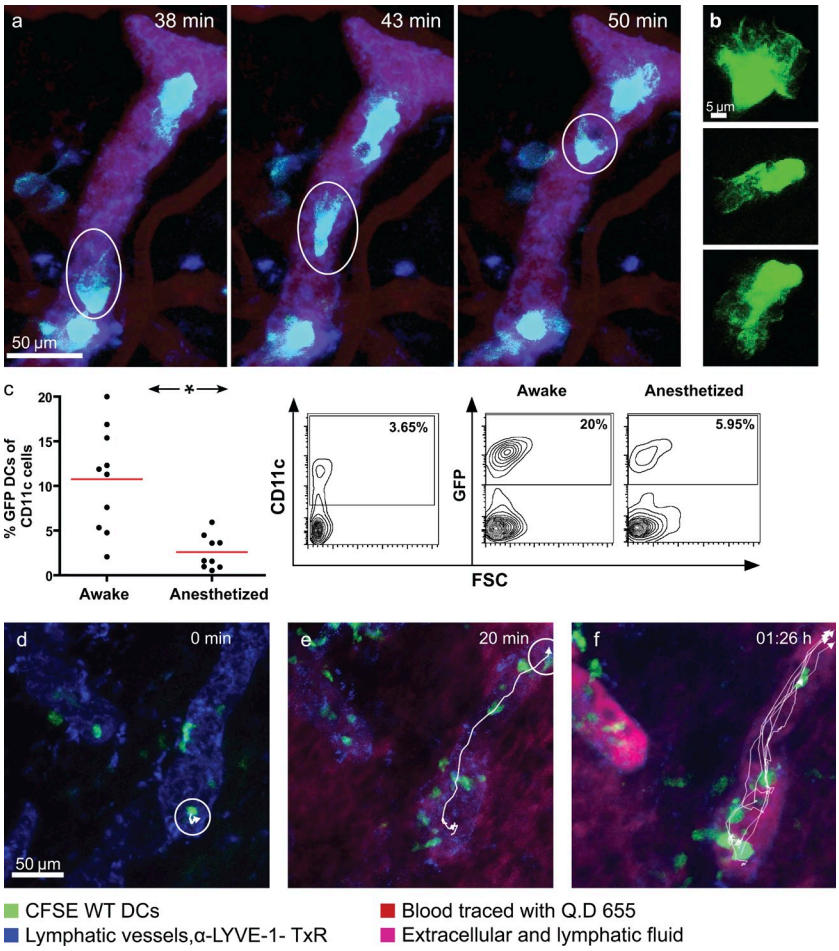

Figure 7. DCs actively crawl inside initial lymphatics using lymph flow as a directional cue. (a) Sequential images of BMDC propagation inside initial lymphatics. Circled is a DC crawling inside the lymphatic lumen. (b) At a higher magnification a DC is seen crawling using lamellipodia at the leading edge and a well defined uropod at the trailing edge. Sequences are representative of at least 13 independent experiments. (c) Under general anesthesia, which is known to reduce lymph flow, the percentage of immigrant GFP+ BMDCs from the footpad skin, as recorded in the popliteal LN 10 h after transfer, drops fivefold ($P < 0.001$). Data represent three independent experiments. Red bars denote the mean. *, $P < 0.001$. (d–f) In the presence of lymph flow, DCs move directionally in the lymphatics. Mice were injected s.c. with 5 µl of fluorescently stained saline (red). As fluid diffused through the interstitium and concentrated in lymphatics, DCs switched from random motility inside lymphatics (d) to directional crawling toward the LN (e). Tracks show several DCs following the same route down the lymphatic vessel (f). Under these conditions DCs crawled along the lymphatic vessel at a mean speed of 9.06 µm/min and a persistence index of 0.65.

has an equally important role as an immobilized ligand. In this form, it primarily promotes leukocyte arrest rather than migration; it triggers T cell arrest on ICAM-1 under flow conditions (Campbell et al., 1998), mediates T cell tethering to DCs (Friedman et al., 2006), and promotes DC adhesion and spread on integrin ligands (Woolf et al., 2007; Schumann et al., 2010). The latter group also proposed a synthesis of these two functions by showing that the immobilized CCL21 can be cleaved by DCs and released to attract more DCs to the T cell zones in LN sections. Here, we present the first in vivo evidence for the crucial role of immobilized CCL21. We suggest, based on the migration patterns of CCR7$^{-/-}$ DCs, that immobilized CCR7 ligands affix DCs to the basal membrane lining the lymphatic endothelium and activate their program for trans-endothelial migration. We support the specific role of CCL21 by ex vivo immunohistology. Conceivably, activated DCs that migrate randomly in the dermis encounter the immobilized chemokine on the basement membrane, dock to it, and generate soluble CCL21 to chemotactically attract more DCs. A potential difficulty is that CCL21 would have to diffuse against the flow of interstitial fluid toward lymphatics (Swartz et al., 2008). The small minority of CCR7$^{-/-}$ DCs that managed to enter lymphatics by bypassing this checkpoint may have used chemokine receptors such as CCR8 (Qu et al., 2004) and CXCR4 (Kabashima et al., 2007) which partially overlap with CCR7 signaling.

After DCs dock to lymphatics, microanatomical structures likely channel their entry into the vessels. In two studies, the group led by M. Sixt recently described the entry of DCs into lymphatics in an explanted preparation of the ear skin (Lämmermann et al., 2008; Pflicke and Sixt, 2009). They showed that DCs cross the basement membrane through preformed portals and then, as suggested previously (Baluk et al., 2007), squeeze through flaps between the button junctions of initial lymphatics. The present study is the first to demonstrate intravitally that several DCs can successively enter through the same portal. It also pinpoints the distribution of CCL21 on initial lymphatics, where chemokine puncta decorate the basal membrane, often next to portals. We propose that CCL21 secreted from the basal aspect of LECs is trapped by collagen type IV in the basement membrane acting as a substrate for DC docking. Additional components may also participate in this process. These include glycosaminoglycans (Hirose et al., 2001; Patel et al., 2001) or podoplanin (Kerjaschki et al., 2004), a glycoprotein expressed selectively on the lymphatic endothelium (Mäkinen et al., 2007).

Rather than acting as an adhesion molecule alone, we suggest that immobilized CCL21 promotes DC adhesion and transmigration by triggering the activation of integrins. The fact that inflammation up-regulates the integrin ligands ICAM-1 and VCAM-1 on lymphatic vessels (Johnson et al., 2006) and that CCL21 promotes DC adhesion to ICAM (Schumann et al., 2010) suggests as much. Our in vitro data,

as well as recent in vitro work using human cells (Johnson and Jackson, 2010), support this scenario directly.

In clinical trials, usually only 5% of injected monocyte-derived DCs reach the draining LN (De Vries et al., 2003). In stark contrast, we typically observe that 95% of LPS-activated BMDCs have entered the lymphatic capillaries 18 h after injection. If one is willing to accept that this finding represents clinical reality, then the rate-limiting step for DC migration from the skin cannot be recruitment into the lymphatics; instead, it might be dispersion within the dermis or crawling in initial lymphatics.

Conducted in intact animals in the presence of lymph flow, our study shows directional cellular motility inside lymphatics. This is the first study to reveal how leukocytes, DCs in this case, propagate in initial lymphatics. We show that lymphatic propagation is hardly the long-imagined passive process produced by hydrodynamic forces. Instead, it requires elaborate crawling guided by a weak lymph current. The simplest interpretation would be that intralymphatic DC migration is essentially random and they are physically pushed downstream by the shear flow of the lymph. Nonetheless, DCs maintained their typical polarized crawling morphology, moved relatively slowly, and departed from their original clusters in a noncoordinated fashion, suggesting directional crawling. It remains unclear how DCs polarize along the lymph flow. Possible mechanisms include integrin-based mechanical sensing of shear forces (Alon and Dustin, 2007) and chemotaxis down an intraluminal gradient of chemokines, perhaps produced by the DCs themselves (Shields et al., 2007; Swartz et al., 2008).

Further complexity is added by a possible change in the profile of CCR7-ligands somewhere along lymphatics, from predominantly CCL21-leu on initial lymphatics to CCL21-ser alone in LN sinuses (Vassileva et al., 1999; Randolph et al., 2005). This transition may manifest itself in the phenotype of *plt* mice, in which CCL21-leu is expressed in peripheral lymphatics but DCs still fail to efficiently migrate into LNs (Gunn et al., 1999; Randolph et al., 2005). We are now using such mice to determine whether lymphatic vessels need to express CCL21 on the luminal surface of their entire length to allow DC migration.

Active DC crawling would have to engage adhesion molecules (such as integrins and their ligands) on both DC and endothelial cell. Many such molecules are up-regulated by inflammatory conditions (Johnson et al., 2006). This additional new step in the course of DC mobilization may thus participate in controlling the rate of DC recruitment to the LN.

Overall, our findings outline a reverse course of events to that observed as leukocytes extravasate into tissues. DCs start by migrating semi-randomly in the dermis, relying on immobilized CCL21 for trans-endothelial migration. In initial lymphatics the lymph current may not be powerful enough to physically push the DCs. The cells overcome this limitation by sensing the direction of flow, polarizing, and actively crawling downstream. In collecting lymphatics (perhaps after a rolling phase that we have not captured yet), DCs switch to passive drifting to exploit the faster flow and reach the draining LN rapidly. Pinpointing the molecular cascades underlying this sequence of events now becomes an interesting course to follow.

MATERIALS AND METHODS

Transgenic mice. Animals were maintained in a specific pathogen-free facility under conditions approved by the institutional animal care and use committee of the Weizmann Institute of Science and the National University of Singapore. Transgenic mice expressing Venus EYFP under the control of the CD11c promoter specifically tagging the DC population were the gift of M. Nussenzweig (The Rockefeller University, New York, NY) and have been previously described (Lindquist et al., 2004). In brief, these mice express high levels of EYFP in all DC populations except plasmacytoid DCs. Expression in other cell populations is too dim to visualize. In the skin, the $EYFP^{hi}$ population consists exclusively of LCs and DDCs (Ng et al., 2008).

The following mouse strains were used in BMDC transfer experiments: (a) BALB/c mice as donors and hosts, (b) $CCR7^{-/-}$ mice back-crossed to C57bl/6 (the gift of S. Lira, Mount Sinai Medical Center, New York, NY) as donors, (c) ubiquitin-EGFP mice (C57BL/6-Tg(UBC-GFP)30Scha/J; The Jackson Laboratory) as donors, and (d) albino tyrosinase-deficient C57BL/6 mice (B6(Cg)-Tyrc-2J/J; The Jackson Laboratory) as hosts.

Induction of inflammation. Footpad inflammation was induced by s.c. injection of 50 µl CFA (Sigma-Aldrich). 24 h after induction of inflammation the footpad was imaged to track the interaction of DDCs with lymphatics.

For whole-mount staining, CHS was achieved by epicutaneous application of a 1:1 mixture of acetone and dibutyl phthalate to the ear skin as described previously (Angeli et al., 2006). Ears were collected for immunohistochemical analysis 24 h after sensitization.

Generation of BMDCs. BMDCs were generated based on a modified established protocol (Lutz et al., 1999). In brief, 4×10^6 cells were cultivated for 13 d in RPMI, supplemented with 10% GM-CSF–conditioned GM-B16 supernatant, which is equivalent to 200 U/ml recombinant mouse GM-CSF (Inaba et al., 1992). One volume of fresh media was added on day 3, and on days 6 and 8 one volume was replaced by fresh media. On day 10, floating cells were transferred to new dishes. Cells were harvested on days 9–13. Analysis of harvested cells revealed that 85–95% expressed CD11c, with 40–60% positive for MHC-II.

Preparation of mice for imaging. Before imaging, mice were anesthetized by i.p injection of 100 mg/kg ketamine + 15 mg/kg xylazine + 2.5 mg/kg acepromazine. Anesthesia was supplemented hourly with half this dose. Mice were placed on a warmed plate and kept at a core temperature of 37°C. The hind paw was placed on a thermally conductive stage (T putty; Laird Technologies) and covered with a glass-bottom imaging chamber.

Live two-photon microscopy of DCs in the skin. We used a microscope (Ultima Multiphoton; Prairie Technologies) incorporating a pulsed laser (Mai Tai Ti-sapphire; Newport Corp.). The laser was tuned to 850 nm to simultaneously excite EYFP and Texas Red, 800 nm to simultaneously excite CFSE and Texas Red, or 880 nm to excite EYFP and Hilyte Fluor 594. A water-immersed 20× (NA 0.95) or 40× (NA 0.8) objective (Olympus) was used. To create a typical time-lapse sequence, a 50-µm-thick section of the dermis containing lymphatic vessels was scanned at 4-µm Z-steps every 30 s.

DC and lymphatic vessel imaging. DCs were labeled with fluorescent dyes. Cells were either incubated in 5% FCS PBS for 5 min with 5 µM CFSE (AnaSpec) at room temperature or with CellTracker blue (Invitrogen) in RPMI for 30 min in 37°. Alternatively, GFP^+ cells were used.

To image initial lymphatics without interfering with DC migration (Gale et al., 2007), we visualized LYVE1. Rat anti–mouse LYVE-1 (clone # 223322; R&D Systems) was covalently conjugated to Texas red or to HiLyte Fluor 594 using labeling kits (AnaSpec). A volume of 50 µl PBS containing

2.5–3.5 × 10^6 DCs, 50 ng LPS (Sigma-Aldrich), and 200 µg anti-LYVE1 was s.c. injected into the hind footpad.

To visualize collecting lymphatics, 30 µl Evans blue (1%; Sigma-Aldrich) was injected s.c. to the hind paw. Lymphatics were followed to the upper shin, and the skin was incised 3 mm below the popliteal LN for visualization.

In vivo DC migration assay. To quantify the efficiency of DC migration to the popliteal LN, we s.c. injected 4 × 10^6 $EGFP^+$ BMDCs to the hind footpad of either awake or continuously anaesthetized mice. LNs were harvested 10 h later and incubated for 45 min at 37°C with 1 mg/ml collagenase D (Roche) diluted in PBS and supplemented with CaCl and MgCl (Sigma-Aldrich). LN cells were then dissociated and analyzed by standard flow cytometry for CD11c (clone N418; BioLegend) and EGFP expression.

Immunostaining. 10-µm-thick cryosections from the skin were prepared as described previously (Lim et al., 2009). For immunohistochemistry, the primary antibodies used included LYVE-1 (rabbit polyclonal, Abcam; or rat clone 223322, R&D systems) and CCL21 (goat polyclonal; R&D Systems). Cy2-conjugated anti–rabbit and Cy3-conjugated anti–goat (Jackson ImmunoResearch Laboratories) were used for detection. Sections were counterstained with DAPI to visualize cell nuclei, and mounted for analysis.

Whole-mount immunohistochemical analysis of ear and footpad skin was performed as described previously (Lim et al., 2009). Mice were perfused with 2% paraformaldehyde, and the tissue was dissected and further fixed in 2% paraformaldehyde overnight at 4°C. Samples were washed, blocked with 0.5% bovine serum albumin and 0.3% Trition X-100 in PBS, and incubated with primary antibodies overnight at 4°C. The antibodies used were directed against LYVE-1 and CCL21 (as in the previous paragraph), VE-cadherin (rat clone 11D4.1; BD), Collagen IV (rabbit polyclonal; Cosmobio), and MHCII (rat clone M5/114.15.2; eBioscience). Secondary antibodies conjugated to Cy2, Cy3, and Dy649 (Jackson ImmunoResearch Laboratories) were used for detection.

Specimens were viewed with a widefield (Axio Imager.Z1; AxioCam HRM camera; Carl Zeiss) or confocal microscope (TCS SP5; Leica) using LAS AF confocal software (version 1.8.2; Leica). Isosurface rendering and confocal z-stacks were processed using Imaris (Bitplane).

Macroscopic lymph flow assessment. To assess the volume of lymph reaching the popliteal LN over 20 min, mice were treated in one footpad with CFA, as described in Induction of inflammation. 24 h later, mice were anesthetized with 1.5% isoflurane and their thighs were shaved for imaging using Xenogen IVIS S100. 40 µl of 70-kD (6.25 mg/ml) Dextran-FITC was injected into each hind footpad. The fluorescent signal of the popliteal LNs was monitored for 30 min and used to determine lymph flow using Living Image software (Xenogen).

Image and statistical analysis. The movement of DCs was analyzed using Volocity software (PerkinElmer). As described before (Lindquist et al., 2004), motion noise was filtered from the data using a minimum movement criterion of 2 µm. Persistence index was calculated as cell displacement divided by path. Arrest coefficient was defined as the proportion of time the cells spent in arrest, i.e., moving slower than 2 µm/min.

A two-tailed Student's *t* test was used to compare the movement parameters in different conditions. The high number of data points (>35) in all experiments ensured normal distribution of the sampling error, relaxing the requirement for equal variance. A p-value <0.05 was considered significant. Whenever significant p-values were reported, nonparametric tests also yielded significant results.

Online supplemental material. Fig. S1 records the presence of $MHC\text{-}II^+$ $EYFP^{hi}$ cells in the dermis. Fig. S2 shows how CFA inflammation in the footpad increases the lymph flow into the popliteal LN. Fig. S3 records passive DC flow in the large collecting lymphatics that collect into the popliteal LN. Video 1 shows optical sectioning of the footpad skin. Video 2 follows DDC motility in the steady state versus inflamed dermis of CD11c-EYFP mice. Video 3 follows DC motility in injured skin. Video 4 follows CD11c-$EYFP^+$ DDCs inside lymphatics. Video 5 demonstrates chemotaxis of BMDCs toward lymphatics and clustering inside them. Video 6 exhibits a three-dimensional reconstruction of a DC contacting CCL21 puncta. Video 7 compares the migration of WT and $CCR7^{-/-}$ DCs in the dermis, pinpointing defects in DC mobilization into lymphatic vessels. Video 8 compares the migration patterns of co-injected WT and $CCR7^{-/-}$ DCs. Video 9 shows trans-endothelial migration of a BMDC into lymphatics. Video 10 captures DC entry through possible preformed portals. Video 11 shows intralymphatic crawling dynamics. Video 12 shows the effects of increased lymph flow on intralymphatic DC crawling. Video 13 shows intralymphatic crawling dynamics under isoflurane anesthesia, Video 14 is a three-dimensional reconstruction of the dispersion of BMDCs in the draining LN. Online supplemental material is available at http://www.jem.org/cgi/content/full/jem.20102392/DC1.

We thank Prof. Ronen Alon and Prof. Steffen Jung for critical discussion.

This work was supported by the Wolfson Family Charitable Trust and by the Minerva Foundation to G. Shakhar and a BMRC grant to V. Angeli.

The authors have no conflicting financial interests.

O. Tal, G. Shakhar, H.Y. Lim, and V. Angeli planned the experiments and wrote the paper. O. Tal and I. Gurevich performed two-photon imaging, tissue culture, and FACS. Z. Shipony, I. Milo, and L.G. Ng participated in image processing and analysis. I. Gurevich prepared BMDCs. H.Y. Lim performed whole-mount staining and confocal microscopy.

Submitted: 15 November 2010
Accepted: 23 August 2011

REFERENCES

Alon, R., and M.L. Dustin. 2007. Force as a facilitator of integrin conformational changes during leukocyte arrest on blood vessels and antigen-presenting cells. *Immunity*. 26:17–27. http://dx.doi.org/10.1016/j.immuni.2007.01.002

Alvarez, D., E.H. Vollmann, and U.H. von Andrian. 2008. Mechanisms and consequences of dendritic cell migration. *Immunity*. 29:325–342. http://dx.doi.org/10.1016/j.immuni.2008.08.006

Angeli, V., F. Ginhoux, J. Llodrà, L. Quemeneur, P.S. Frenette, M. Skobe, R. Jessberger, M. Merad, and G.J. Randolph. 2006. B cell-driven lymphangiogenesis in inflamed lymph nodes enhances dendritic cell mobilization. *Immunity*. 24:203–215. http://dx.doi.org/10.1016/j.immuni.2006.01.003

Baluk, P., J. Fuxe, H. Hashizume, T. Romano, E. Lashnits, S. Butz, D. Vestweber, M. Corada, C. Molendini, E. Dejana, and D.M. McDonald. 2007. Functionally specialized junctions between endothelial cells of lymphatic vessels. *J. Exp. Med.* 204:2349–2362. http://dx.doi.org/10.1084/jem.20062596

Banchereau, J., and R.M. Steinman. 1998. Dendritic cells and the control of immunity. *Nature*. 392:245–252. http://dx.doi.org/10.1038/32588

Bedoui, S., P.G. Whitney, J. Waithman, L. Eidsmo, L. Wakim, I. Caminschi, R.S. Allan, M. Wojtasiak, K. Shortman, F.R. Carbone, et al. 2009. Cross-presentation of viral and self antigens by skin-derived CD103+ dendritic cells. *Nat. Immunol.* 10:488–495. http://dx.doi.org/10.1038/ni.1724

Brewig, N., A. Kissenpfennig, B. Malissen, A. Veit, T. Bickert, B. Fleischer, S. Mostböck, and U. Ritter. 2009. Priming of CD8+ and CD4+ T cells in experimental leishmaniasis is initiated by different dendritic cell subtypes. *J. Immunol.* 182:774–783.

Britschgi, M.R., S. Favre, and S.A. Luther. 2010. CCL21 is sufficient to mediate DC migration, maturation and function in the absence of CCL19. *Eur. J. Immunol.* 40:1266–1271. http://dx.doi.org/10.1002/eji.200939921

Campbell, J.J., J. Hedrick, A. Zlotnik, M.A. Siani, D.A. Thompson, and E.C. Butcher. 1998. Chemokines and the arrest of lymphocytes rolling under flow conditions. *Science*. 279:381–384. http://dx.doi.org/10.1126/science.279.5349.381

Cavanagh, L.L., and W. Weninger. 2008. Dendritic cell behaviour in vivo: lessons learned from intravital two-photon microscopy. *Immunol. Cell Biol.* 86:428–438. http://dx.doi.org/10.1038/icb.2008.25

Czeloth, N., G. Bernhardt, F. Hofmann, H. Genth, and R. Förster. 2005. Sphingosine-1-phosphate mediates migration of mature dendritic cells. *J. Immunol.* 175:2960–2967.

Dadiani, M., V. Kalchenko, A. Yosepovich, R. Margalit, Y. Hassid, H. Degani, and D. Seger. 2006. Real-time imaging of lymphogenic metastasis in orthotopic human breast cancer. *Cancer Res.* 66:8037–8041. http://dx.doi.org/10.1158/0008-5472.CAN-06-0728

De Vries, I.J., D.J. Krooshoop, N.M. Scharenborg, W.J. Lesterhuis, J.H. Diepstra, G.N. Van Muijen, S.P. Strijk, T.J. Ruers, O.C. Boerman, W.J. Oyen, et al. 2003. Effective migration of antigen-pulsed dendritic cells to lymph nodes in melanoma patients is determined by their maturation state. *Cancer Res.* 63:12–17.

Dieu, M.C., B. Vanbervliet, A. Vicari, J.M. Bridon, E. Oldham, S. Aït-Yahia, F. Brière, A. Zlotnik, S. Lebecque, and C. Caux. 1998. Selective recruitment of immature and mature dendritic cells by distinct chemokines expressed in different anatomic sites. *J. Exp. Med.* 188:373–386. http://dx.doi.org/10.1084/jem.188.2.373

Förster, R., A. Schubel, D. Breitfeld, E. Kremmer, I. Renner-Müller, E. Wolf, and M. Lipp. 1999. CCR7 coordinates the primary immune response by establishing functional microenvironments in secondary lymphoid organs. *Cell.* 99:23–33. http://dx.doi.org/10.1016/S0092-8674(00)80059-8

Friedman, R.S., J. Jacobelli, and M.F. Krummel. 2006. Surface-bound chemokines capture and prime T cells for synapse formation. *Nat. Immunol.* 7:1101–1108. http://dx.doi.org/10.1038/ni1384

Gale, N.W., R. Prevo, J. Espinosa, D.J. Ferguson, M.G. Dominguez, G.D. Yancopoulos, G. Thurston, and D.G. Jackson. 2007. Normal lymphatic development and function in mice deficient for the lymphatic hyaluronan receptor LYVE-1. *Mol. Cell. Biol.* 27:595–604. http://dx.doi.org/10.1128/MCB.01503-06

Germain, R.N., M.J. Miller, M.L. Dustin, and M.C. Nussenzweig. 2006. Dynamic imaging of the immune system: progress, pitfalls and promise. *Nat. Rev. Immunol.* 6:497–507. http://dx.doi.org/10.1038/nri1884

Gunn, M.D., S. Kyuwa, C. Tam, T. Kakiuchi, A. Matsuzawa, L.T. Williams, and H. Nakano. 1999. Mice lacking expression of secondary lymphoid organ chemokine have defects in lymphocyte homing and dendritic cell localization. *J. Exp. Med.* 189:451–460. http://dx.doi.org/10.1084/jem.189.3.451

Harrell, M.I., B.M. Iritani, and A. Ruddell. 2008. Lymph node mapping in the mouse. *J. Immunol. Methods.* 332:170–174. http://dx.doi.org/10.1016/j.jim.2007.11.012

Hayashi, K., P. Jiang, K. Yamauchi, N. Yamamoto, H. Tsuchiya, K. Tomita, A.R. Moossa, M. Bouvet, and R.M. Hoffman. 2007. Real-time imaging of tumor-cell shedding and trafficking in lymphatic channels. *Cancer Res.* 67:8223–8228. http://dx.doi.org/10.1158/0008-5472.CAN-07-1237

Helft, J., F. Ginhoux, M. Bogunovic, and M. Merad. 2010. Origin and functional heterogeneity of non-lymphoid tissue dendritic cells in mice. *Immunol. Rev.* 234:55–75. http://dx.doi.org/10.1111/j.0105-2896.2009.00885.x

Hirose, J., H. Kawashima, O. Yoshie, K. Tashiro, and M. Miyasaka. 2001. Versican interacts with chemokines and modulates cellular responses. *J. Biol. Chem.* 276:5228–5234. http://dx.doi.org/10.1074/jbc.M007542200

Inaba, K., M. Inaba, N. Romani, H. Aya, M. Deguchi, S. Ikehara, S. Muramatsu, and R.M. Steinman. 1992. Generation of large numbers of dendritic cells from mouse bone marrow cultures supplemented with granulocyte/macrophage colony-stimulating factor. *J. Exp. Med.* 176:1693–1702. http://dx.doi.org/10.1084/jem.176.6.1693

Itano, A.A., S.J. McSorley, R.L. Reinhardt, B.D. Ehst, E. Ingulli, A.Y. Rudensky, and M.K. Jenkins. 2003. Distinct dendritic cell populations sequentially present antigen to CD4 T cells and stimulate different aspects of cell-mediated immunity. *Immunity.* 19:47–57. http://dx.doi.org/10.1016/S1074-7613(03)00175-4

Johnson, L.A., and D.G. Jackson. 2010. Inflammation-induced secretion of CCL21 in lymphatic endothelium is a key regulator of integrin-mediated dendritic cell transmigration. *Int. Immunol.* 22:839–849. http://dx.doi.org/10.1093/intimm/dxq435

Johnson, L.A., S. Clasper, A.P. Holt, P.F. Lalor, D. Baban, and D.G. Jackson. 2006. An inflammation-induced mechanism for leukocyte transmigration across lymphatic vessel endothelium. *J. Exp. Med.* 203:2763–2777. http://dx.doi.org/10.1084/jem.20051759

Kabashima, K., N. Shiraishi, K. Sugita, T. Mori, A. Onoue, M. Kobayashi, J. Sakabe, R. Yoshiki, H. Tamamura, N. Fujii, et al. 2007. CXCL12-CXCR4 engagement is required for migration of cutaneous dendritic cells. *Am. J. Pathol.* 171:1249–1257. http://dx.doi.org/10.2353/ajpath.2007.070225

Kamath, A.T., S. Henri, F. Battye, D.F. Tough, and K. Shortman. 2002. Developmental kinetics and lifespan of dendritic cells in mouse lymphoid organs. *Blood.* 100:1734–1741.

Kelly, R.H., B.M. Balfour, J.A. Armstrong, and S. Griffiths. 1978. Functional anatomy of lymph nodes. II. Peripheral lymph-borne mononuclear cells. *Anat. Rec.* 190:5–21. http://dx.doi.org/10.1002/ar.1091900103

Kerjaschki, D., H.M. Regele, I. Moosberger, K. Nagy-Bojarski, B. Watschinger, A. Soleiman, P. Birner, S. Krieger, A. Hovorka, G. Silberhumer, et al. 2004. Lymphatic neoangiogenesis in human kidney transplants is associated with immunologically active lymphocytic infiltrates. *J. Am. Soc. Nephrol.* 15:603–612. http://dx.doi.org/10.1097/01.ASN.0000113316.52371.2E

Kissenpfennig, A., S. Henri, B. Dubois, C. Laplace-Builhé, P. Perrin, N. Romani, C.H. Tripp, P. Douillard, L. Leserman, D. Kaiserlian, et al. 2005. Dynamics and function of Langerhans cells in vivo: dermal dendritic cells colonize lymph node areas distinct from slower migrating Langerhans cells. *Immunity.* 22:643–654. http://dx.doi.org/10.1016/j.immuni.2005.04.004

Lämmermann, T., B.L. Bader, S.J. Monkley, T. Worbs, R. Wedlich-Söldner, K. Hirsch, M. Keller, R. Förster, D.R. Critchley, R. Fässler, and M. Sixt. 2008. Rapid leukocyte migration by integrin-independent flowing and squeezing. *Nature.* 453:51–55. http://dx.doi.org/10.1038/nature06887

Ley, K., C. Laudanna, M.I. Cybulsky, and S. Nourshargh. 2007. Getting to the site of inflammation: the leukocyte adhesion cascade updated. *Nat. Rev. Immunol.* 7:678–689. http://dx.doi.org/10.1038/nri2156

Lim, H.Y., J.M. Rutkowski, J. Helft, S.T. Reddy, M.A. Swartz, G.J. Randolph, and V. Angeli. 2009. Hypercholesterolemic mice exhibit lymphatic vessel dysfunction and degeneration. *Am. J. Pathol.* 175:1328–1337. http://dx.doi.org/10.2353/ajpath.2009.080963

Lindquist, R.L., G. Shakhar, D. Dudziak, H. Wardemann, T. Eisenreich, M.L. Dustin, and M.C. Nussenzweig. 2004. Visualizing dendritic cell networks in vivo. *Nat. Immunol.* 5:1243–1250. http://dx.doi.org/10.1038/ni1139

Lutz, M.B., N. Kukutsch, A.L. Ogilvie, S. Rössner, F. Koch, N. Romani, and G. Schuler. 1999. An advanced culture method for generating large quantities of highly pure dendritic cells from mouse bone marrow. *J. Immunol. Methods.* 223:77–92. http://dx.doi.org/10.1016/S0022-1759(98)00204-X

Mäkinen, T., C. Norrmén, and T.V. Petrova. 2007. Molecular mechanisms of lymphatic vascular development. *Cell. Mol. Life Sci.* 64:1915–1929. http://dx.doi.org/10.1007/s00018-007-7040-z

Martín-Fontecha, A., S. Sebastiani, U.E. Höpken, M. Uguccioni, M. Lipp, A. Lanzavecchia, and F. Sallusto. 2003. Regulation of dendritic cell migration to the draining lymph node: impact on T lymphocyte traffic and priming. *J. Exp. Med.* 198:615–621. http://dx.doi.org/10.1084/jem.20030448

Merad, M., F. Ginhoux, and M. Collin. 2008. Origin, homeostasis and function of Langerhans cells and other langerin-expressing dendritic cells. *Nat. Rev. Immunol.* 8:935–947. http://dx.doi.org/10.1038/nri2455

Miller, M.J., O. Safrina, I. Parker, and M.D. Cahalan. 2004. Imaging the single cell dynamics of $CD4^+$ T cell activation by dendritic cells in lymph nodes. *J. Exp. Med.* 200:847–856. http://dx.doi.org/10.1084/jem.20041236

Miteva, D.O., J.M. Rutkowski, J.B. Dixon, W. Kilarski, J.D. Shields, and M.A. Swartz. 2010. Transmural flow modulates cell and fluid transport functions of lymphatic endothelium. *Circ. Res.* 106:920–931. http://dx.doi.org/10.1161/CIRCRESAHA.109.207274

Ng, L.G., A. Hsu, M.A. Mandell, B. Roediger, C. Hoeller, P. Mrass, A. Iparraguirre, L.L. Cavanagh, J.A. Triccas, S.M. Beverley, et al. 2008. Migratory dermal dendritic cells act as rapid sensors of protozoan parasites. *PLoS Pathog.* 4:e1000222. http://dx.doi.org/10.1371/journal.ppat.1000222

Ohl, L., M. Mohaupt, N. Czeloth, G. Hintzen, Z. Kiafard, J. Zwirner, T. Blankenstein, G. Henning, and R. Förster. 2004. CCR7 governs skin dendritic cell migration under inflammatory and steady-state conditions. *Immunity.* 21:279–288. http://dx.doi.org/10.1016/j.immuni.2004.06.014

Patel, D.D., W. Koopmann, T. Imai, L.P. Whichard, O. Yoshie, and M.S. Krangel. 2001. Chemokines have diverse abilities to form solid phase gradients. *Clin. Immunol.* 99:43–52. http://dx.doi.org/10.1006/clim.2000.4997

Pflicke, H., and M. Sixt. 2009. Preformed portals facilitate dendritic cell entry into afferent lymphatic vessels. *J. Exp. Med.* 206:2925–2935. http://dx.doi.org/10.1084/jem.20091739

Proudfoot, A.E., T.M. Handel, Z. Johnson, E.K. Lau, P. LiWang, I. Clark-Lewis, F. Borlat, T.N. Wells, and M.H. Kosco-Vilbois. 2003. Glycosaminoglycan binding and oligomerization are essential for the in vivo activity of certain chemokines. *Proc. Natl. Acad. Sci. USA.* 100:1885–1890. http://dx.doi.org/10.1073/pnas.0334864100

Qu, C., E.W. Edwards, F. Tacke, V. Angeli, J. Llodrá, G. Sanchez-Schmitz, A. Garin, N.S. Haque, W. Peters, N. van Rooijen, et al. 2004. Role of CCR8 and other chemokine pathways in the migration of monocyte-derived dendritic cells to lymph nodes. *J. Exp. Med.* 200:1231–1241. http://dx.doi.org/10.1084/jem.20032152

Randolph, G.J., V. Angeli, and M.A. Swartz. 2005. Dendritic-cell trafficking to lymph nodes through lymphatic vessels. *Nat. Rev. Immunol.* 5:617–628. http://dx.doi.org/10.1038/nri1670

Romani, N., M. Thurnher, J. Idoyaga, R.M. Steinman, and V. Flacher. 2010. Targeting of antigens to skin dendritic cells: possibilities to enhance vaccine efficacy. *Immunol. Cell Biol.* 88:424–430. http://dx.doi.org/10.1038/icb.2010.39

Saeki, H., A.M. Moore, M.J. Brown, and S.T. Hwang. 1999. Cutting edge: secondary lymphoid-tissue chemokine (SLC) and CC chemokine receptor 7 (CCR7) participate in the emigration pathway of mature dendritic cells from the skin to regional lymph nodes. *J. Immunol.* 162:2472–2475.

Schmid-Schönbein, G.W. 1990. Microlymphatics and lymph flow. *Physiol. Rev.* 70:987–1028.

Schumann, K., T. Lämmermann, M. Bruckner, D.F. Legler, J. Polleux, J.P. Spatz, G. Schuler, R. Förster, M.B. Lutz, L. Sorokin, and M. Sixt. 2010. Immobilized chemokine fields and soluble chemokine gradients cooperatively shape migration patterns of dendritic cells. *Immunity.* 32:703–713. http://dx.doi.org/10.1016/j.immuni.2010.04.017

Sen, D., L. Forrest, T.B. Kepler, I. Parker, and M.D. Cahalan. 2010. Selective and site-specific mobilization of dermal dendritic cells and Langerhans cells by Th1- and Th2-polarizing adjuvants. *Proc. Natl. Acad. Sci. USA.* 107:8334–8339. http://dx.doi.org/10.1073/pnas.0912817107

Shields, J.D., M.E. Fleury, C. Yong, A.A. Tomei, G.J. Randolph, and M.A. Swartz. 2007. Autologous chemotaxis as a mechanism of tumor cell homing to lymphatics via interstitial flow and autocrine CCR7 signaling. *Cancer Cell.* 11:526–538. http://dx.doi.org/10.1016/j.ccr.2007.04.020

Swartz, M.A., J.A. Hubbell, and S.T. Reddy. 2008. Lymphatic drainage function and its immunological implications: from dendritic cell homing to vaccine design. *Semin. Immunol.* 20:147–156. http://dx.doi.org/10.1016/j.smim.2007.11.007

Vassileva, G., H. Soto, A. Zlotnik, H. Nakano, T. Kakiuchi, J.A. Hedrick, and S.A. Lira. 1999. The reduced expression of 6Ckine in the *plt* mouse results from the deletion of one of two 6Ckine genes. *J. Exp. Med.* 190:1183–1188. http://dx.doi.org/10.1084/jem.190.8.1183

Woolf, E., I. Grigorova, A. Sagiv, V. Grabovsky, S.W. Feigelson, Z. Shulman, T. Hartmann, M. Sixt, J.G. Cyster, and R. Alon. 2007. Lymph node chemokines promote sustained T lymphocyte motility without triggering stable integrin adhesiveness in the absence of shear forces. *Nat. Immunol.* 8:1076–1085. http://dx.doi.org/10.1038/ni1499

Yang, B.G., T. Tanaka, M.H. Jang, Z. Bai, H. Hayasaka, and M. Miyasaka. 2007. Binding of lymphoid chemokines to collagen IV that accumulates in the basal lamina of high endothelial venules: its implications in lymphocyte trafficking. *J. Immunol.* 179:4376–4382.

Zinselmeyer, B.H., J.N. Lynch, X. Zhang, T. Aoshi, and M.J. Miller. 2008. Video-rate two-photon imaging of mouse footpad - a promising model for studying leukocyte recruitment dynamics during inflammation. *Inflamm. Res.* 57:93–96. http://dx.doi.org/10.1007/s00011-007-7195-y